(18) Svanholm, U.; Parker, V. D. *Acta Chem. Scand.* **1973**, *27*, 1454–1456.
(19) Padilla, A. G.; Wu, S. M.; Shine, H. J. *J. Chem. Soc., Chem. Commun.* **1976**, 236–237.
(20) Evans, B.; Smith, K. M.; Cavaleiro, J. A. S. *J. Chem. Soc., Perkin Trans. 1* **1978**, 768–773.
(21) Perrin, D. D. "Dissociation Constants of Organic Bases in Aqueous Solution", Butterworth: London, 1965.
(22) Chakrabarty, M. R.; Handloser, C. S.; Mosher, M. W. *J. Chem. Soc., Perkin Trans. 2* **1973**, 938–942.
(23) Besecke, S.; Evans, B.; Barnett, G. H.; Smith, K. M.; Fuhrhop, J.-H. *Angew. Chem.* **1976**, *88*, 616.
(24) Koyama, K.; Susuki, T.; Tsutsumi, S. *Tetrahedron Lett.* **1965**, 627–630.
(25) Nilsson, S. *Acta Chem. Scand.* **1973**, *27*, 329–335.
(26) Shine, H. J.; Ristagno, C. V. *J. Org. Chem.* **1972**, *37*, 3424–3426.
(27) Inhoffen, H. H. Fuhrhop, J.-H., Voigt, H.; Brockmann, H. *Justus Liebigs Ann. Chem.* **1966**, *695*, 133–143.
(28) Grigg, R.; Shelton, G.; Sweeney, A.; Johnson, A. W. *J. Chem. Soc., Perkin Trans. 1* **1972**, 1789–1799.
(29) Fanning, J. C.; Gray, T. L. *J. Chem. Soc., Chem. Commun.* **1974**, 23–24.
(30) Wittig, G.; Geissler, G. *Justus Liebigs Ann. Chem.* **1953**, *580*, 44–57.
(31) Maercker, A., *Org. React.* **1965**, *14*, 270–490.
(32) Clezy, P. S.; Fookes, C. J. R. *J. Chem. Soc., Chem. Commun.* **1971**, 1268.
(33) Bonnett, R.; Charalambides, A. C.; Martin, R. A. *J. Chem. Soc., Perkin Trans. 1* **1978**, 974–980.
(34) (a) Jackson, A. H.; Kenner, G. W.; McGillivray, G.; Smith, K. M. *J. Chem. Soc. C* **1968**, 294–302. (b) Barnett, G. H.; Hudson, M. F.; McCombie, S. W.; Smith, K. M. *J. Chem. Soc., Perkin Trans. 1* **1973**, 691–696.
(35) Cavaleiro, J. A. S.; Smith, K. M. *J. Chem. Soc., Perkin Trans. 1* **1973**, 2149–2155.
(36) Evans, B.; Smith, K. M. *Tetrahedron* **1977**, *33*, 629–633.
(37) Fajer, J.; Borg, D. C.; Forman, A.; Felton, R. H.; Vegh, L.; Dolphin, D. *Ann. N.Y. Acad. Sci.* **1973**, *206*, 349–363.
(38) Cox, M. T.; Howarth, T. T.; Jackson, A. H.; Kenner, G. W., *J. Am. Chem. Soc.* **1969**, *91*, 1232–1233.
(39) Kochi, J. K.; Bethea, III, T. W. *J. Org. Chem.* **1968**, *33*, 75–82.
(40) E.g., Svanholm, U.; Parker, V. D. *J. Am. Chem. Soc.* **1976**, *98*, 997–1001, 2942–2946.
(41) Abraham, R. J.; Eivazi, F.; Pearson, H.; Smith, K. M. *J. Chem. Soc., Chem. Commun.* **1976**, 698–699, 699–701.
(42) Fuhrhop, J.-H.; Wasser, P.; Reisner, D.; Mauzerall, D. *J. Am. Chem. Soc.* **1972**, *94*, 7996–8001. Fajer, J.; Borg, D. C.; Forman, A.; Dolphin, D.; Felton, R. H. *Ibid.* **1970**, *92*, 3451–3459.
(43) Dolphin, D.; Halko, D. J.; Johnson, E. C.; Rousseau, K. In "Porphyrin Chemistry Advances", Longo, F. R., Ed.; Ann Arbor Press: Ann Arbor, Mich., 1979; pp 119–141.
(44) Fuhrhop, J.-H.; Mauzerall, D. *J. Am. Chem. Soc.* **1969**, *91*, 4174–4181.
(45) Smith, K. M. *J. Chem. Soc., Perkin Trans. 1* **1972**, 1471–1475.
(46) Whitlock, H. W.; Hanauer, R. W.; Oester, M. Y.; Bower, B. K. *J. Am. Chem. Soc.* **1969**, *91*, 7485–7489.
(47) Johnson, A. W.; Oldfield, D. *J. Chem. Soc. C* **1965**, 4303–4312.

A Unified Mechanism for Thermal and Photochemical Activation of Charge-Transfer Processes with Organometals. Steric Effects in the Insertion of Tetracyanoethylene

S. Fukuzumi, K. Mochida, and J. K. Kochi*

Contribution from the Department of Chemistry, Indiana University, Bloomington, Indiana 47401. *Received February 5, 1979*

Abstract: Transient absorption bands observed with organometals and the common electron acceptor, tetracyanoethylene (TCNE), are shown to arise from 1:1 charge-transfer complexes. The frequency of the charge-transfer band ν_{CT}, as well as the formation constant K_{CT} and extinction coefficient ϵ_{CT}, of weak σ-π complexes derived from a series of homologous tetraalkyltin compounds R_4Sn are sensitive measures of electronic and steric effects, as determined independently by the ionization potentials I_D and the steric parameters of alkyl groups E_s, respectively, of the donor. The disappearance of the charge-transfer (CT) complex follows overall second-order kinetics with rate constant k_T, and it leads to the 1:1 insertion adduct $R_3Sn(TCNE)R$. The same adduct can also be produced with unit quantum yield by the direct irradiation of the charge-transfer band at low temperatures where the thermal reaction does not occur. Steric effects in the formation of the complex (K_{CT}) parallel those in the thermal insertion (k_T). Steric effects are reflected in the photochemical insertion insofar as they influence the energy and oscillator strength of the CT transition as well as the formation constant of the complex. Thermal activation ($\log k_T$) and photochemical activation ($h\nu_{CT}$) of insertion are both associated with an electron-transfer process which proceeds from the charge-transfer complex [R_4Sn TCNE] to form the same paramagnetic ion pair [$R_4Sn^+ \cdot TCNE^- \cdot$]. Thermal and photochemical processes also share common intermediates subsequent to activation by electron transfer. Thus, in both, insertion follows from a series of rapid, dark reactions involving the stepwise collapse of the ion pair [$R_4Sn^+ \cdot TCNE^- \cdot$] by (1) the spontaneous fragmentation of the $R_4Sn^+ \cdot$ moiety akin to that observed in the gas phase upon electron impact, followed by (2) radical recombination and ion pairing all within the solvent cage. The nature of the ion pair is probed by examining selectivities in mixed methylethyltin compounds for Me-Sn and Et-Sn insertions. The alkyl and TCNE radical pair, that is, [$R \cdot R_3Sn^+ TCNE^- \cdot$], is shown to be the prime intermediate by quantum-yield measurements for their simultaneous formation during the irradiation of the charge-transfer band in a frozen matrix at −175 °C. No CIDNP could be observed during thermal activation of insertion.

Introduction

Organometals are involved as reactants or intermediates in a variety of synthetic organic procedures and catalytic processes. As electron-rich species, they are generally subject to cleavage by acids, metal complexes, and other electrophiles.[1] Furthermore, alkylmetals can have rather low ionization potentials, and electron-transfer mechanisms are also possible in which the rate is limited by the ability of the organometal to function as an electron donor and the electrophile to be an electron acceptor.

Tetracyanoethylene (TCNE) has been widely used as an electron acceptor in charge transfer spectral studies, particularly with organic π donors.[2] Donor-acceptor interactions with TCNE have been reported for a few organometallic σ donors.[3-6] The charge-transfer bands for organometals RM are generally weak, and more interestingly they are transient, leading to the simple 1:1 adduct, i.e.

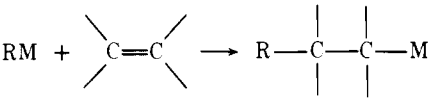

(1)

0002-7863/79/1501-5961$01.00/0

Table I. Formation and Reaction of Charge-Transfer Complexes of Alkyltin and Tetracyanoethylene[a]

no.	alkyltin	I_D, eV	λ_{max}, nm	ν_{CT}, 10^{-4} cm^{-1}	ϵ_{CT}, M^{-1} cm^{-1}	K_{CT}, M^{-1} [b]	k_T, M^{-1} s^{-1} [b]
1	Me_4Sn	9.69	345	2.90	500	0.17 (−0.76)	1.5×10^{-5} (−4.82)
2	Et_4Sn	8.90	421	2.38	167	0.53 (−0.28)	8.6×10^{-4} (−3.07)
3	*n*-Pr_4Sn	8.82	415	2.41	29	2.2 (0.34)	2.6×10^{-3} (−2.59)
4	*n*-Bu_4Sn	8.76	416	2.40	16	7.7 (0.89)	9.1×10^{-3} (−2.04)
5	$EtMe_3Sn$		373	2.68	222	0.24 (−0.61)	9.2×10^{-5} (−4.04)
6	*n*-$PrMe_3Sn$	9.1	360	2.78	200	0.25 (−0.61)	2.0×10^{-5} (−4.70)
7	*n*-$BuMe_3Sn$		352	2.84	172	0.21 (−0.68)	2.9×10^{-5} (−4.54)
8	Et_2Me_2Sn	9.01	381	2.62	143	0.80 (−0.10)	4.6×10^{-4} (−3.34)
9	*n*-Pr_2Me_2Sn	8.8	388	2.58	77	1.5 (0.16)	4.3×10^{-4} (−3.37)
10	*n*-Bu_2Me_2Sn	8.8	386	2.59	50	1.1 (0.04)	6.3×10^{-4} (−3.20)
11	*i*-Pr_4Sn	8.46	437	2.29	95	1.0 (0.0)	1.4×10^{-3} (−2.85)
12	*sec*-Bu_4Sn	8.45	430	2.33	71	2.5 (0.39)	6.1×10^{-3} (−2.21)
13	*i*-Bu_4Sn	8.68	415	2.41	125	0.30 (−0.52)	2.2×10^{-4} (−3.66)
14	*i*-$PrMe_3Sn$	8.9	405	2.47	40	1.0 (0.0)	6.5×10^{-4} (−3.19)
15	*t*-$BuMe_3Sn$	8.6	425	2.35			6.6×10^{-3} (−2.18)
16	*i*-Pr_2Me_2Sn	8.56	421	2.38	118	0.95 (−0.02)	1.2×10^{-3} (−2.92)
17	*t*-Bu_2Me_2Sn	8.22	421	2.38	77	0.65 (−0.19)	3.7×10^{-4} (−3.43)
18	*i*-Bu_2Et_2Sn		421	2.38	143	0.40 (−0.40)	3.3×10^{-4} (−3.48)
19	*neo*-$Pent_3EtSn$						7.3×10^{-5} (−4.14)
20	*neo*-$Pent_4Sn$	8.67					no reaction

[a] Charge-transfer spectra measured in chloroform solution at 25 °C; second-order rate constants measured in acetonitrile at 25 °C. [b] Logarithms in parentheses.

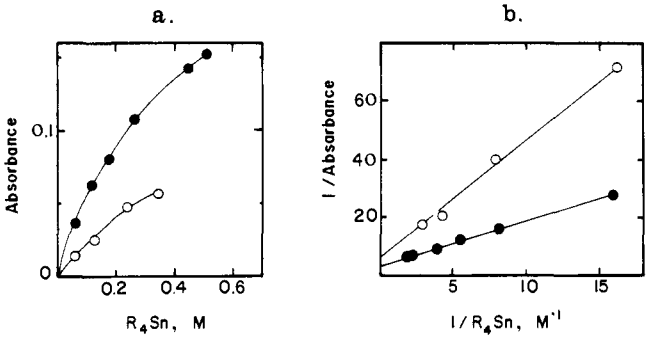

Figure 1. (a) Absorbance of the charge-transfer spectrum of *n*-Pr_4Sn and TCNE in (○) 1,1-dichloropropane solution, λ_{max} 412 nm, and (●) chloroform at 415 nm. (b) Benesi-Hildebrand plot of (a).

Insertion as described in eq 1 is relatively common with organometals in a variety of stoichiometric and catalytic processes.[7,8] We believe that, as a prototype, the mechanism of insertion, in which the alkyl-metal bond is broken and TCNE inserted, merits detailed attention. Indeed, the recent observation[9] that the same insertion reaction can also be promoted by direct irradiation of the charge-transfer band presents the rare opportunity of examining the interrelationship between the electronic excitation and the thermal chemical reactions attendant upon charge-transfer interaction. Although spectroscopic studies of charge-transfer interactions are common, there are only a limited number of chemical effects arising from molecular complexing,[10] and to our knowledge no examples in which electronic transitions have been intimately interrelated with the chemical processes.

A variety of alkylmetal structures are available, and in this study we chose a series of tetraalkyltin compounds which differ principally in their donor properties as well as their steric effects, in order to probe the effect of the driving force and the intermolecular separation on charge-transfer processes. We first measure the magnitudes of the formation constants of the charge-transfer complexes between tetraalkyltin and TCNE, and describe their properties in relation to steric effects. The role of charge-transfer complexes in the thermal insertion reaction is then shown by establishing its relationship to photochemical activation. Steric effects provide a useful mechanistic probe, common to both.

Results

Charge-Transfer Spectra of Alkyltin–TCNE Complexes. Determination of K_{CT} and ϵ_{CT}. New absorption bands are observed in the visible region immediately upon mixing a chloroform or 1,2-dichloropropane solution of TCNE with tetraalkyltin compounds.

$$R_4Sn + TCNE \overset{K_{CT}}{\rightleftharpoons} [R_4Sn\ TCNE] \qquad (2)$$

The bands are broad, as is characteristic of intermolecular charge-transfer spectra,[2] and the absorption maxima are highly dependent on the structure of the tetraalkyltin compounds listed in Table I. The absorbance increases with the concentrations of both TCNE and alkyltin as shown in Figure 1a. The use of relatively high concentrations of alkyltin (~0.1 M) and TCNE (~0.01 M) was necessitated by the rather low absorbances. Indeed, the [R_4Sn TCNE] complexes are expected to have low formation constants since they may be considered as σ-π complexes arising from a charge-transfer interaction between the σ HOMO of R_4Sn and the π LUMO of TCNE.

Generally for weak charge-transfer complexes such as these, it is often difficult to obtain separate values of the formation constant K_{CT} and the extinction coefficient ϵ_{CT} from a Benesi-Hildebrand plot of the data represented in spectrophotometric form for the absorbance A as

$$\frac{C_0}{A} = \frac{1}{K_{CT}\epsilon_{CT}}\frac{1}{D_0} + \frac{1}{\epsilon_{CT}} \qquad (3)$$

where C_0 and D_0 are the initial concentrations of the acceptor and donor, respectively, for unit cell path length.[2,11] The slope and intercept reflect K_{CT} and ϵ_{CT}, respectively, but as $K_{CT} \rightarrow 0$, then $K_{CT}D_0 \ll 1$ and only the $K_{CT}\epsilon_{CT}$ product can be determined. However, for the tetraalkyltin-TCNE complexes, the clear, positive intercepts shown in Figure 1b for tetra-*n*-propyltin, a typical example, can be attributed to the relatively small values of ϵ_{CT} (vide infra). In this region, however, the question as to whether the charge-transfer absorption is due to 1:1 complexes or a contact pair of contiguous molecules[12] is difficult to resolve experimentally. This point is especially

relevant since the values of K_{CT} in Table I do not parallel ϵ_{CT}, as predicted from simple orbital overlap considerations.[13] On the contrary, the opposite trend appears to pertain. Such a deviation has also been observed in iodine complexes with methylbenzenes,[14] and led Orgel and Mulliken[15] to suggest the contribution from contacts, for which K_{CT} lacks physical significance.[16,17] To establish whether the values of K_{CT} and ϵ_{CT} obtained by the Benesi-Hildebrand method for [R_4Sn TCNE] represent real values for charge-transfer complexes, we reevaluated them by an independent method utilizing the disappearance of TCNE in 1,2-dichloropropane solutions.

When $[R_4Sn]_0 \gg [TCNE]_0$ and $1 \gg K_{CT}[R_4Sn]_0$, the concentration of the charge-transfer complex [R_4Sn TCNE] is given by

$$[R_4Sn\ TCNE] = K_{CT}[R_4Sn]_0[TCNE]_0 \qquad (4)$$

Since $[TCNE]_0 = [TCNE] + [R_4Sn\ TCNE]$, the spectrophotometric form of eq 4 is given by

$$\frac{A'_0}{A'} - 1 = K_{CT}[R_4Sn]_0 \qquad (5)$$

where A'_0 and A' represent the initial and final absorbance of the relatively intense π-π^* band of TCNE at 270 nm (ϵ 15 500 M^{-1} cm^{-1}).[18] Indeed, the absorbance changes immediately upon mixing the tetraalkyltin and TCNE solutions. The plot of eq 5 shown in Figure 2 is linear, and it passes through the origin. The value of K_{CT} measured by the slope is independent of the concentration of TCNE.[19,20] Tetra-*n*-propyltin and diethyldiisobutyltin, shown in Figures 2a and 2b, respectively, were chosen as representative examples of tetraalkyltin compounds since they have rather extreme values of K_{CT}.

The values of K_{CT} = 1.7 and 0.24 for tetra-*n*-propyltin and diethyldiisobutyltin, respectively, obtained by this technique accord well with the values of 1.5 and 0.27 obtained from the Benesi-Hildebrand method. We conclude that the charge-transfer spectra observed with tetraalkyltin compounds and TCNE are due to 1:1 complexes. Albeit weakly formed, they are to be distinguished from 1:1 contacts. Furthermore, the values of K_{CT} listed in Table I for various tetraalkyltin compounds accord with the criterion proposed by Person[22] [viz., $0.1 < K_{CT}D_0$] for the distinction between very weak charge-transfer complexes and contacts.

The charge-transfer band is transient, and the rate of its decay depends on the structure of the alkyltin compound. The disappearance of the charge-transfer band coincides with the formation of the adducts as described in the next section.

Insertion Reactions of Tetraalkyltin and Tetracyanoethylene. Thermal Processes. Homoleptic alkylmetals derived from tin, lead, and mercury react with TCNE to afford 1:1 adducts which have been characterized as products of TCNE insertion into an alkylmetal bond.[5] For tetraalkyltin compounds, the insertion reaction is represented as eq 6. The course of reaction

$$R_4Sn + (NC)_2C{=}C(CN)_2 \xrightarrow{k_T} R_3Sn{-}\underset{NC}{\overset{NC}{C}}{-}\underset{CN}{\overset{CN}{C}}{-}R \qquad (6)$$

can be followed readily by changes in the ^1H NMR spectrum. For example, the reaction of tetramethyltin and TCNE in acetonitrile-d_3 was sufficiently slow to allow simultaneous observation of the disappearance of Me_4Sn (δ 0.09 singlet, 12 H) and the concomitant appearance of the trimethyltin (δ 0.69 singlet, 9 H) and methyl (δ 2.16 singlet, 3 H) resonances of the insertion product. TCNE inserts cleanly into only one Sn-Me bond. Line broadening in the NMR spectrum due to the adventitious formation of TCNE anion radical (vide infra) can be eliminated by the use of 10% v acetic-d_3 acid-d_1. The kinetics and selectivity of the insertion process, as well as the

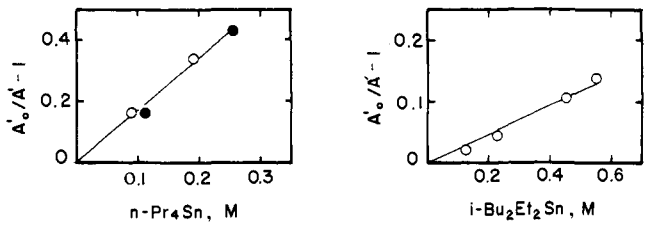

Figure 2. Alternate determination of K_{CT} from the change in TCNE concentration according to eq 5. Left: (○) 4.7 × 10^{-4} *M* and (●) 7.9 × 10^{-4} M TCNE in 1,2-dichloropropane at 270, 258, or 280 nm. Right: (○) 1.1 × 10^{-3} M TCNE.

ESR spectra of $R_3SnTCNE$ radicals and attempts to observe chemically induced dynamic polarization, are described separately below.

1. Kinetics of the Thermal Process. The rate of insertion was followed spectrophotometrically by the disappearance of the TCNE at 270 nm. The kinetics of the reaction were determined by varying the concentrations, and showed a first-order dependence on each reactant.

$$-\frac{d[TCNE]}{dt} = k_T[R_4Sn][TCNE] \qquad (7)$$

The second-order rate constants k_T are listed in Table I for a series of alkyltin compounds. The largest rate constant was observed with *t*-$BuSnMe_3$, but the rate of the highly hindered tetraneopentyltin was too slow to be observed.

The rate of insertion depends on the polarity of the solvent. Thus, the rates increase on proceeding from hydrocarbon solvents, such as toluene and hexane, to methylene chloride and to acetonitrile, roughly in the order of their increasing solvent polarity parameters, determined by the E_T^* and Z values.[2a] The solvent, the second-order rate constant at 37 °C, and the E_T^* values of the solvent at 25 °C follow: toluene, 1.2 × 10^{-4} M^{-1} s^{-1}, 33.9 kcal mol^{-1}; hexane (containing 0.2% v acetonitrile for solubility), 7 × 10^{-6} M^{-1} s^{-1}, 30.9 kcal mol^{-1} (for pure hexane); methylene chloride, 1.8 × 10^{-3} M^{-1} s^{-1}, 42 kcal mol^{-1}; acetonitrile, 4.7 × 10^{-3} M^{-1} s^{-1}, 46 kcal mol^{-1} for tetraethyltin. The temperature dependence of the insertion rate for tetramethyltin and TCNE in acetonitrile solution affords the apparent activation parameters, $\Delta H^{\ddagger}$ = 10 kcal mol^{-1} and $\Delta S^{\ddagger}$ = −11 eu.

2. Selectivity Studies in the Thermal Insertion of Methylethyltin Compounds. Selectivity in the insertion of TCNE into tetraalkyltin compounds is determined from the relative yields of the isomeric adducts. For dimethyldiethyltin, insertion affords two adducts, I and II, corresponding to intramolecular competition between Me-Sn and Et-Sn cleavage, respectively. The relative yields of I and II in Table II were determined from their ^1H NMR spectra as described in the Experimental Section. The selectivity for ethyl/methyl cleavage $S(Et/Me)$ is then given by k_{Et}/k_{Me} in eq 8. After correction for the statis-

$$Me_2SnEt_2 + TCNE \xrightarrow{k_{Me}} Me(NC)_2CC(CN)_2SnMeEt_2 \quad (8a)$$
$$\text{I}$$
$$Me_2SnEt_2 + TCNE \xrightarrow{k_{Et}} Et(NC)_2CC(CN)_2SnMe_2Et \quad (8b)$$
$$\text{II}$$

tical factor, ethyltrimethyltin shows essentially the same selectivity $S(Et/Me)$ as that derived from dimethyldiethyltin. Similar selectivities are also qualitatively observed with other mixed tetraalkyltin compounds, in which insertion occurs preferentially into the weakest alkyl-tin bond.

3. Formation of Radicals from TCNE. When tetra-*sec*-butyltin is added to TCNE in 1,2-dichloropropane solution, the appearance of the stable radical derived from TCNE can be readily detected by its ESR spectrum consisting of nine

Table II. Selectivity in the Thermal Insertion with Methylethyltin Compounds[a]

$Et_nMe_{4-n}Sn$, M	TCNE, M	time, h	temp, °C	$S(Et/Me)^b$
		Et_2Me_2Sn		
0.16	0.16	21	22	9
0.64	0.64	2	40	10
0.16	0.16	7	40	9
		$EtMe_3Sn$		
0.16	0.16	3.5	22	12
0.16	0.16	7	22	10
0.16	0.16	11	22	10
0.16	0.16	27	22	9
0.16	0.16	7	40	11
0.64	0.64	2	40	11

[a] In CD_3CN solutions. [b] Selectivity for Me_3EtSn includes statistical correction.

broad lines centered at $g = 2.0030$. At relatively low modulations, the spectrum is further resolved into 45 lines, which can be assigned to the TCNE radical IIIa (M = *sec*-Bu_3Sn),

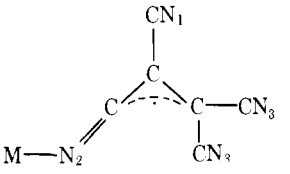

III

showing coupling to three magnetically nonequivalent nitrogen nuclei ($a_{N_1} = 1.21$, $a_{N_2} = 2.05$, and $a_{N_{3,3}} = 1.75$ G). Indeed, the magnitudes of these hyperfine splittings are similar to those observed in the tributyltin analogue derived from hexabutylditin and TCNE.[23] [Furthermore, the well-resolved spectrum of the pentacarbonylmanganese derivative assigned as IIIb, where M = $Mn(CO)_5$, was strongly supported by a simulated spectrum with $a_{N_1} = 1.201$, $a_{N_2} = 2.530$, $a_{N_{3,3}} = 1.734$ G.] However, the relative intensities of the lines for the species derived from alkyltin do not accord with that expected for simply IIIa. Similar abnormalities in line intensities have been observed in the ESR spectra of related magnesium derivatives, and may be due to structural fluctuations in labile ion pairs (such as R_3Sn^+ $TCNE^-\cdot$).[24-26] The ESR spectrum measured at 77 K is anisotropic, consisting of nine broad lines under low modulation ($g_\parallel = 2.0025 \pm 0.0001$, $A_\parallel = 5.48 \pm 0.10$ G; $g_\perp = 2.0036 \pm 0.0001$, $A_\perp \sim 0$). The hyperfine components of the anisotropic spectrum are similar to those observed with the alkali salts of TCNE anion radical.[27] Unfortunately, the broad ESR lines under these more or less anisotropic conditions do not allow the structure of the radical species to be distinguished between either free $TCNE^-\cdot$ or IIIa.

4. Chemically Induced Dynamic Polarization (CIDNP) Studies. The ^1H NMR spectra of the reactant and the adducts showed neither emission nor enhanced absorption when the reaction of tetraalkyltin compounds with TCNE was carried out at 35 °C in the probe of the spectrometer. However, with this system there remains the possibility that the insertion occurs too slowly to detect the steady-state CIDNP spectra. For this reason, the related insertions[5] of the more reactive tetraethyllead and dimethyldiethyllead were also examined, since they react with TCNE on mixing at this temperature. Furthermore, at −30 °C the reactions are sufficiently slow to observe the buildup of insertion products, but deemed fast enough to detect CIDNP effects if they should pertain. No unusual features of the NMR spectra were observed. Finally, the effect of magnetic field strength was also examined by the prior mixing of the reactants in the earth's magnetic field (~0.5 G) or in a permanent magnetic field (300 G) and at various distances outside the magnetic field (23 kG) of the probe. No CIDNP was detected, although the observations previously reported[28] could be repeated.

Table III. Quantum Yields for Insertion of Tetraalkyltin and TCNE by Irradiation at 436 nm[a]

alkyltin, M	TCNE, M	irradiation time, h	insertion[b] adduct, 10^3 M	light[c]	Q^c
		Me_4Sn			
0.32	0.31	5	3.9	3.6	1.1
0.32	0.16	10	6.9	7.3	1.0
0.64	0.31	10	7.9	7.3	1.1
		Et_4Sn			
0.15	0.015	2	0.80[d]	0.72	1.1

[a] At −35 °C in acetonitrile solution. [b] Determined by NMR. [c] Apparent quantum yield determined by yield of adduct divided by light intensity and time. [d] Determined by change in TCNE concentration. [e] In units of 10^3 einstein L^{-1}.

Photochemically Induced Insertion of Tetraalkyltin and TCNE. In order to show that the thermally induced insertion of TCNE into tetraalkyltin can also be induced photochemically, we examined a system under conditions in which the thermal process was too slow to observe.

1. Quantum Yields for Photoinsertion. Tetramethyltin undergoes no appreciable reaction with TCNE in acetonitrile solutions at −35 °C. However, irradiation of this solution at 436 nm afforded the same 1:1 adduct, previously described in eq 6 (R = Me) for the thermal process (eq 9). Insertion induced

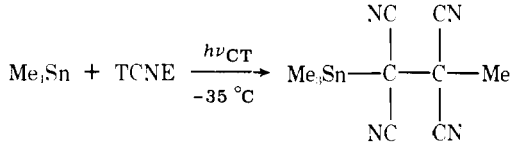

photochemically at this wavelength proceeds with unit quantum yield, independent of the initial concentration of tetraalkyltin or TCNE. The same result is obtained with tetraethyltin as listed in Table III. Neither TCNE nor tetramethyltin shows any significant absorption in this region.

2. Observation of Alkyl Radicals and TCNE Anion Radical during Irradiation of the CT Band in Rigid Media. Alkyl radicals are generated during irradiation of the charge-transfer band of the [R_4Sn TCNE] complex. For example, a quartz tube of a degassed solution of di-*tert*-butyldimethyltin and TCNE in a mixed solvent consisting of 1:1 v/v acetonitrile and 1,2-dichloropropane was placed in the ESR cavity and frozen at −175 °C. Subsequent irradiation in situ afforded the ESR spectrum in Figure 3, showing the somewhat broadened, but clearly resolved, spectrum of the *tert*-butyl radical ($g = 2.0027$, $a_H = 22.8 \pm 0.1$ G)[29] superimposed on that of the TCNE anion radical. The central "line" of the spectrum representing the envelope of the unresolved spectrum of the TCNE anion radical can be partially resolved at lower modulations as shown in the upper right inset. All ten lines of the *tert*-butyl radical are also clearly discernible, the $m_I = -9/2$ and $-7/2$ lines being shown at higher gain in the upper left inset. The ESR spectrum of the *tert*-butyl radical is stable at this temperature. However, it disappears within 5 min if the matrix is annealed at −140 °C. No *tert*-butyl radical is observed in the absence of TCNE.

The series of time-lapse spectra shown in Figure 4 were taken at constant temperature and under constant irradiation through a filter transmitting in a narrow band (436 nm) close to the maximum (421 nm) of the charge-transfer absorption. The simultaneous growth of *tert*-butyl radical and TCNE anion radical are plotted in Figure 5, which shows that they are formed at essentially the same rate.

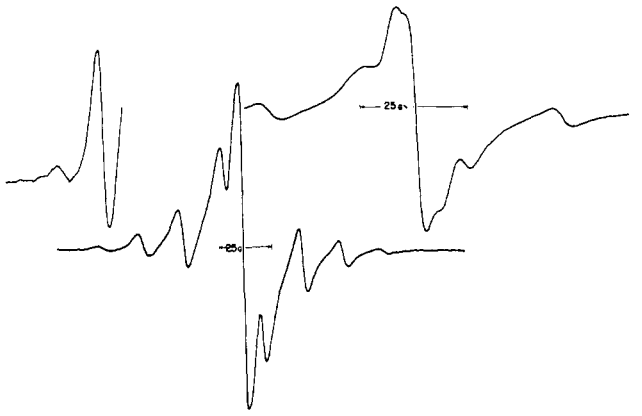

Figure 3. The ESR spectrum obtained from the irradiation through a Pyrex filter of a 1:1 mixture of *t*-Bu_2Me_2Sn and TCNE in 50% acetonitrile and 1,2-dichloropropane at −175 °C. Upper left inset at higher gain (×10) showing resolved $m_I = -9/2$ and $-7/2$ lines of the *tert*-butyl radical. Upper right inset at higher resolution (×4) and lower gain (×1/8) shows the partial resolution of the "central" line due to TCNE radical (displaced from $g = 2.003$) by irradiation through a 436-nm filter.

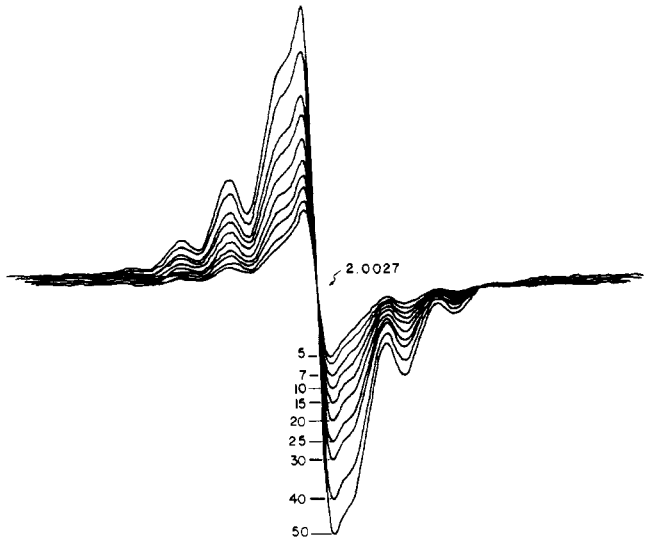

Figure 4. The time dependence of the ESR spectrum derived from a 1:1 mixture of *t*-Bu_2Me_2Sn and TCNE in 50% v acetonitrile and 1,2-dichloropropane at −175 °C by constant irradiation through a 436-nm filter. Times shown in minutes.

$$[t\text{-}Bu_2SnMe_2\ TCNE] \xrightarrow[-175\ °C]{h\nu CT} [t\text{-}Bu\cdot\ t\text{-}BuSnMe_2^+\ TCNE^{-}\cdot] \quad (10)$$

The wavelength dependence for the formation of *tert*-butyl and TCNE radicals was also examined close to the low- and high-energy edges of the charge-transfer band shown in Figure 6. (The bandwidths of the filters used are superimposed on the charge-transfer spectrum.) The results in column 7 of Table IV show that *tert*-butyl and TCNE radicals are both formed with quantum yields of about 0.2, independent of the wavelength of incident light. However, additional TCNE radical is produced upon irradiation at the high-energy end of the charge-transfer band, since the quantum yield at 262 nm is 0.55. In the absence of TCNE no *tert*-butyl radicals can be observed upon irradiation, and without *t*-Bu_2SnMe_2 no TCNE radical was detected.

Irradiation at 436 nm of the charge-transfer complex of *tert*-butyltrimethyltin and TCNE also leads to the simultaneous formation of *tert*-butyl and TCNE radical, but with slightly diminished quantum yields. No methyl radical was observed. Although ethyl radicals were readily generated from tetraethylgermane, attempts to observe the alkyl radicals from tetraethyltin, tetraisobutyltin, and tetra-*sec*-butyltin under similar conditions were unsuccessful.

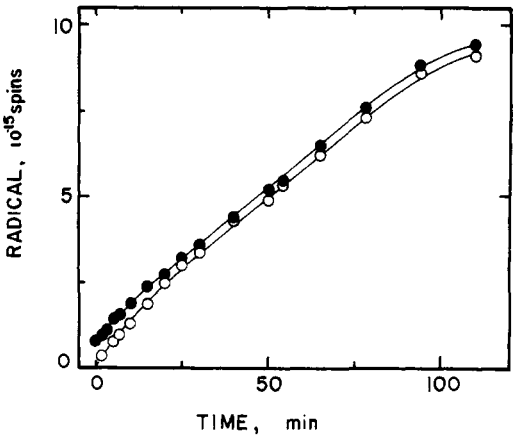

Figure 5. Simultaneous formation of (○) *t*-Bu· and (●) $TCNE^{-}\cdot$ upon irradiation at 436 nm of 0.21 M *t*-Bu_2Me_2Sn and 0.16 M TCNE in 1:1 CH_3CN-1,2-dichloropropane at −175 °C.

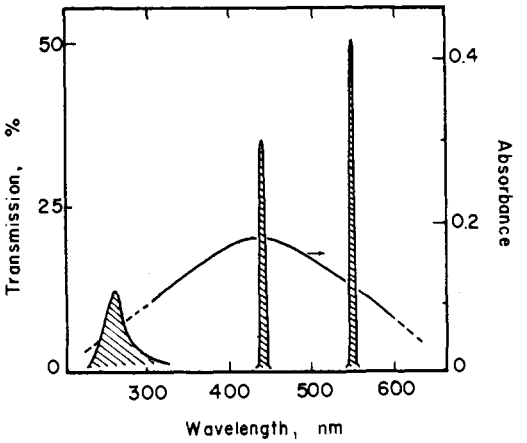

Figure 6. Charge-transfer spectrum of 0.39 M *t*-Bu_2Me_2Sn and 0.010 M TCNE in chloroform, superimposed on the transmission characteristics of various interference filters employed.

Table IV. Rate of Formation of *tert*-Butyl Radical and TCNE Anion Radical by Constant Irradiation of *tert*-Butyltin Compounds at −175 °C

tert-butyltin, M	TCNE, M	filter[a]	d[TCNE⁻·]/dt 10^{-14} spm[b]	d[*t*-Bu·]/dt 10^{-14} spm	I_0, 10^{-14} qpm	Q^c
			t-Bu_2Me_2Sn			
0.21	0.16	262	1.1	0.51	2.0	0.25
0.21	0.16	436	1.1	1.1	5.3	0.21
0.21	0.66	546	0.11	0.11	0.54	0.20
0.42	0.039	436	0.11	0.11	5.3	0.021
0.42	0.031	436	0.082	0.083	5.3	0.016
0.42	0.016	436	0.056	0.057	5.3	0.011
0.42	0.0094	436	0.030	0.032	5.3	0.006
0.42	0.0031	436	0.022	0.022	5.3	0.004
			t-$BuMe_3Sn$			
0.26	0.31	436	1.7	1.7	16.4	0.10
0.52	0.31	436	2.1	2.0	16.4	0.12

[a] For transmission characteristics see Figure 6. [b] Spins per minute. [c] Apparent quantum yield for *tert*-butyl radical obtained from column 5 divided by I_0.

Table V. Selectivities in the Photochemical Insertion of Alkyltin and TCNE[a]

alkyltin, M	TCNE, M	irradiation time, h	conversion, %	Q^b	S(Et/Me)
		Me_3SnEt			
0.30	0.31	17	27	0.8	11
0.30	0.31	31	40	0.7	9
		Me_2SnEt_2			
0.30	0.31	17	37	1	6
0.30	0.31	31	48	0.8	8

[a] In CD_3CN solution at −40 °C. [b] Yield of product divided by light intensity and time. Compare Tables II and III.

3. Selectivity Studies in the Photochemical Insertion of Methylethyltin Compounds. In order to compare the photoinduced insertion of TCNE into alkyltin with the thermal process, the selectivity was redetermined for the same series of methylethyltin compounds used in Table II, i.e., eq 11. The

$$Et_2SnMe_2 + TCNE \xrightarrow{h\nu_{CT}} \begin{cases} \xrightarrow{k_{Et}} Et(NC)_2CC(CN)_2SnMe_2Et & (11a) \\ \xrightarrow{k_{Me}} Me(NC)_2CC(CN)_2SnEt_2Me & (11b) \end{cases}$$

irradiation was carried out at −40 °C, however, to prevent interference from the thermal insertion. Within experimental uncertainties, the selectivity S(Et/Me) as described by the ratio k_{Et}/k_{Me} of the two photoprocesses in eq 11 is the same as that determined for the thermal processes in eq 8. Table V shows that essentially the same results were obtained for Me_3EtSn after statistical correction.

Ionization Potentials and Mass Spectral Cracking Patterns of Tetraalkyltin Compounds. The ionization potentials of the tetraalkyltin compounds used in this study were determined in the gas phase from their photoelectron spectra.[30] Electron detachment in tetraalkyltin compounds, i.e.

$$R_4Sn \xrightarrow{-e} R_4Sn^{+}\cdot$$

proceeds from a carbon-tin, σ-bonding orbital,[31a] similar to that described for dialkylmercury compounds.[31b]

The fragmentation pattern of tetraalkyltin compounds upon electron impact also derives from the parent molecule ion.[32] Selectivities in the series of methylethyltin compounds, e.g.

$$Me_2SnEt_2 \xrightarrow{-e} Me_2SnEt_2^{+}\cdot, \text{ etc.}$$

reflect fragmentation of methyl and ethyl radicals. At an ionizing voltage of 20 eV (nominal), the higher alkyl homologues in the series $RSnMe_3$ undergo preferential loss of the alkyl group in the order Me < Et ≃ *n*-Pr ≃ *n*-Bu < *i*-Pr < *t*-Bu approximately as 1:6:7:8:14:19 in accord with the decreasing trend in the alkyl-tin bond energies.

Discussion

The mechanistic study of the insertion reaction for alkyltin and TCNE merits special attention since it represents a rare example of a charge-transfer process in which thermal as well as photochemical activation can be separately identified and subjected to detailed examination. Indeed, we wish to show that the availability of these dual pathways allows (1) the charge-transfer complex to be established as common to both and (2) the activation process whether it occurs thermally or photochemically to be identified as electron transfer to afford the paramagnetic ion pair, i.e.

$$[R_4Sn\ TCNE] \xrightarrow{\Delta \text{ or } h\nu} [R_4Sn^{+}\cdot\ TCNE^{-}\cdot] \qquad (12)$$

which is formally akin to that previously studied with iron(III) and iridate(IV) oxidants,[33] e.g.

$$[R_4Sn\ Ir^{IV}Cl_6^{2-}] \rightarrow [R_4Sn^{+}\cdot\ Ir^{III}Cl_6^{3-}] \qquad (13)$$

Since the charge-transfer complex of alkyltin and TCNE plays an important role in insertion, we wish to first focus on their formation and properties, particularly with regard to steric effects. We then follow with a stepwise description of photochemical and thermal activation of electron transfer within the complex, and how it leads to insertion.

Steric Effects in the Formation of Charge-Transfer Complexes of Alkyltin and TCNE. The formation of weak charge-transfer complexes of alkyltin and TCNE in eq 2 is characterized by an optical transition, $h\nu_{CT}$, for the electron-transfer process described in eq 12. Under these circumstances, the frequency of the charge-transfer band measured in the gas phase can be approximated by

$$h\nu_{CT} = I_D - E_A - e^2/\bar{r}_{D,A} \qquad (14)$$

where I_D and E_A refer to the vertical ionization potential of the donor (tetraalkyltin) and the electron affinity of the acceptor (TCNE), respectively.[34] The electrostatic term includes $\bar{r}_{D,A}$, which is related to the mean intermolecular separation in the CT complex. The influence of steric effects on the alkyltin-TCNE complexes is manifested in both the energy ν_{CT} as well as the intensity ϵ_{CT} of the charge-transfer band as described below.

1. Frequency of the Charge-Transfer Transition. According to eq 14, if $\bar{r}_{D,A}$ remains unchanged for a series of similar alkylmetals interacting with a common acceptor such as TCNE, ν_{CT} should be linearly related to the ionization potentials. Indeed, this correlation, shown in Figure 7, is excellent for two-coordinate dialkylmercury compounds, spanning a range of more than 40 kcal mol^{-1} from dimethylmercury at one end to di-*tert*-butylmercury at the other.[35] The plot for tetraalkyltin compounds shows the same general trend, but with considerable scatter of the data. A comparison of the correlations for dialkylmercury and tetraalkyltin shows two additional striking differences. At the same values of the ionization potentials, the charge-transfer bands for tetraalkyltin consistently lie to higher energies of those for dialkylmercury. The difference may be qualitatively attributed to smaller values of $\bar{r}_{D,A}$ in eq 14 allowed by the open, linear dialkylmercury in comparison to the quasi-spherical, tetrahedral tetraalkyltin.[36] The same geometrical factor may account for the apparent absence of a steric effect in the charge-transfer frequencies with dialkylmercury, since the highly branched di-*tert*-butylmercury is well included in the linear correlation. On the other hand, a detailed inspection of the data for tetraalkyltin shows that the scatter of points can be attributed to a consistent trend of deviations due to steric effects. Thus, if we take the slope of the mercury correlation as a guide, the deviations always increase to the high-energy side of ν_{CT} in the order *t*-Bu > *i*-Pr > Et > Me for α-methyl substitution and *i*-Bu > *n*-Pr > Et for β-methyl substitution.[37,38] Indeed ν_{CT} for tetraneopentyltin, which is the most sterically encumbered compound examined, may lie in the ultraviolet well beyond that of tetramethyltin despite its much lower ionization potential (8.67 eV).

2. Comments on K_{CT} and ϵ_{CT}. The formation constants K_{CT} of charge-transfer complexes generally increase with the intensity of the absorption bands, since the transition dipole (proportional to $\epsilon_{CT}^{1/2}$) is related to the orbital overlap.[13] However, in the alkyltin-TCNE complexes, no such relation is apparent from the listing of K_{CT} and ϵ_{CT} in Table I. For example, in the symmetric R_4Sn, K_{CT} increases regularly in

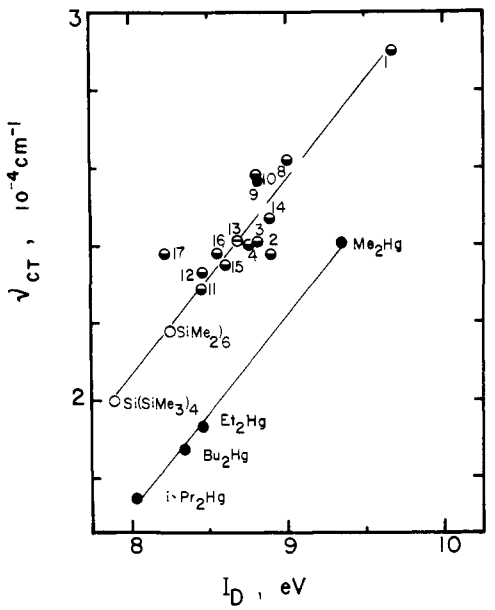

Figure 7. Correlation of the frequency of the charge-transfer band with the ionization potentials of alkylmetals: (●) R_2Hg, (⊖) R_4Sn (listed by numbers in Table I), (○) $(SiMe_2)_6$ and $Si(SiMe_3)_4$ from ref 3.

Table VI

R = alkyltin	Me		Et		*n*-Pr		*n*-Bu	
	K_{CT}	ϵ_{CT}	K_{CT}	ϵ_{CT}	K_{CT}	ϵ_{CT}	K_{CT}	ϵ_{CT}
R_4Sn	0.17	500	0.53	167	2.2	29	7.7	16
R_2SnMe_2	0.17	500	0.80	143	1.5	7.7	1.1	50
$RSnMe_3$	0.17	500	0.24	222	0.25	200	0.21	172

the order Me < Et < *n*-Pr < *n*-Bu while ϵ_{CT} decreases in the same order. Similarly, for the mixed methylalkyltin compounds R_nSnMe_{4-n}, the same opposing trends of K_{CT} and ϵ_{CT} pertain as presented in Table VI.

The coulombic term in eq 14 cannot simply account for the inverse correlation between K_{CT} and ϵ_{CT} since the values of ν_{CT} for Et_4Sn, *n*-Pr_4Sn, and *n*-Bu_4Sn are rather constant. We propose that the inverse correlation derives from steric effects which impose constraints on the intermolecular distances $\bar{r}_{D,A}$ and $\bar{r}_{D^+A^-}$ in the charge-transfer complex and the ion pair, respectively. The potential energy surfaces are drawn in Figure 8 with a crossover region ($\bar{r}_{D^+A^-} < \bar{r}_{D,A}$)[39,40] to allow the thermal electron transfer from the charge-transfer complex in eq 12 to be an adiabatic process. The charge-transfer band, denoted as $h\nu_{CT}$, is associated with the transition from the ground vibrational state to a higher vibrational state of the excited complex. We attribute the rather small values of ϵ_{CT} primarily to the low probability associated with the vibrational contribution to the total transition probability.[41,42] As steric constraints cause larger changes in the intermolecular distances, particularly $\bar{r}_{D,A} - \bar{r}_{D^+A^-}$, the excitation will become increasingly forbidden as it occurs to higher quantum levels in the vibrational manifold. Thus, for the series of straight-chain alkyl derivatives R_nSnMe_{4-n} discussed above, as $\bar{r}_{D,A}$ increases with chain length it will lead to decreases in ϵ_{CT}; the parallel increase in K_{CT} follows from the trend in I_D in accord with charge-transfer theory. As steric hindrance continues to increase, particularly as a result of alkyl branching, $\bar{r}_{D,A}$ will increase further, and the electrostatic term, $e^2/\bar{r}_{D,A}$, will diminish in importance. The net result could even be a decrease in $\bar{r}_{D,A} - \bar{r}_{D^+A^-}$, leading to an increase in ϵ_{CT} as suggested for the series in Table VII. The complex interplay of electrostatic and steric effects precludes a simple relationship between the

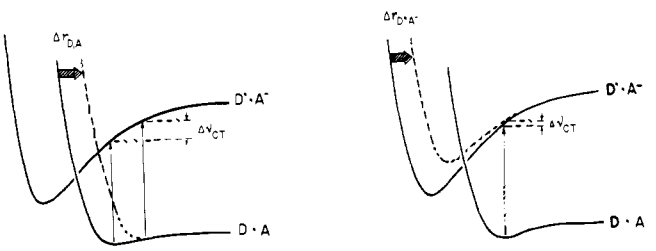

Figure 8. Schematic illustration of steric influences on intermolecular separations in the ion pair (right) and the charge-transfer complex (left) and the effect on changes in charge-transfer frequencies.

Table VII

R_2SnMe_2	R = *n*-Pr(*n*-Bu)	*i*-Pr	*i*-Bu	*t*-Bu
K_{CT}	1.5 (1.1)	0.95	0.40	0.65
ϵ_{CT}	77 (50)	118	143	77

formation constant of the charge-transfer complex and the extinction coefficient for these highly branched, mixed alkyltin compounds.

Mechanism of Insertion. Thermal and Photochemical Processes. The observation of the charge-transfer complex of alkyltin and TCNE does not, by itself, prove that the complex lies along the reaction pathway to insertion. Complex formation may represent an unrelated side reaction. The difference lies in whether the rate-limiting, second-order rate constant k_T for electron transfer is a product, $K_{CT}k_{et}$, as represented in the equations

$$R_4Sn + TCNE \overset{K_{CT}}{\rightleftharpoons} [R_4Sn\ TCNE] \qquad (15)$$

$$[R_4Sn\ TCNE] \xrightarrow{k_{et}} [R_4Sn^+\cdot\ TCNE^-\cdot] \qquad (16)$$

or a simple bimolecular constant representing the direct reaction of alkyltin and TCNE, distinct from the charge-transfer complex as in the equation

$$[R_4Sn\ TCNE] \overset{K_{CT}}{\rightleftharpoons} R_4Sn + TCNE$$

$$\xrightarrow{k_{et}} R_4Sn^+\cdot + TCNE^-\cdot \qquad (17)$$

Although the distinction may be largely meaningless for charge-transfer reactions in general as Colter and Dack[43] have pointed out, we believe that electron transfer proceeds directly from the alkyltin-TCNE complex. The reasons derive from (1) the correlation of the formation constant K_{CT} with the phenomenological rate constant k_T, as well as the intimate relationship between (2) the photochemical activation and (3) the thermal activation of electron transfer. Following a discussion of these mechanistic points, we wish to consider (4) the nature and fate of the ion pair as an intermediate common to both thermal and photochemical activation and (5) steric effects involved in the electron transfer within the charge-transfer complex.

1. Correlation of K_{CT} and k_T for the Thermal Reaction. The measured second-order rate constant k_T for the reaction of alkyltin and TCNE is plotted against the formation constant K_{CT} for the charge-transfer complex in Figure 9. Despite the absence of any correlation of K_{CT} with the ionization potential I_D of tetraalkyltin or the frequency ν_{CT} of the charge-transfer complex due to steric effects as discussed above, there is a reasonable correlation with the overall second-order rate constant. Such a parallel relationship between K_{CT} and k_T is more in keeping with the charge-transfer complex as an intermediate, rather than as an unrelated side product.[44]

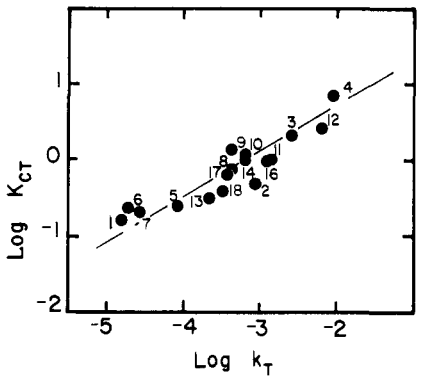

Figure 9. The parallel between formation constants of charge-transfer complexes and the thermal rates of insertion. Numbers refer to tetraalkyltin compounds in Table I.

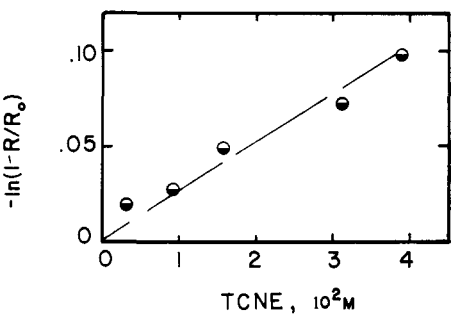

Figure 10. Production of *tert*-butyl radicals resulting from the irradiation of the charge-transfer band of t-Bu_2Me_2Sn and TCNE according to eq 21 and the data in Table IV.

2. Photochemical Activation of Insertion. Photoinsertion, resulting from irradiation directly at 436 or at 546 nm, where only the charge-transfer absorption occurs, must necessarily proceed via excitation of the charge-transfer complex and not that of either alkyltin or TCNE alone.

$$[R_4Sn\ TCNE] \xrightarrow{h\nu_{CT}} [R_4Sn^+ \cdot\ TCNE^- \cdot] \qquad (18)$$

Moreover, the ESR studies described by eq 10 and in Figure 5 demonstrate that alkyl radicals and TCNE anion radicals are intermediates formed simultaneously during this photoactivation. They must result from a dark reaction following electron transfer, i.e.

$$[R_4Sn^+ \cdot\ TCNE^- \cdot] \xrightarrow{\text{fast}} [R \cdot\ R_3Sn^+\ TCNE^- \cdot] \qquad (19)$$

in accord with the known instability of the tetraalkyltin cation radical.[30]

The lifetime of the pair of caged radicals in eq 19 is exceedingly short, and their direct ESR observation is only allowed by the physical constraints imposed by the frozen matrix. Indeed, the quantum yields reported in Table IV do not adequately reflect the efficiency of radical production since a certain amount of cage combination is doubtlessly taking place prior to observation. Even under these conditions radical production can be directly related to charge-transfer excitation. Thus, the rate of a photochemical reaction is generally given by[45]

$$R = I_0\Phi(1 - e^{-2.3\epsilon Cd}) = R_0(1 - e^{-2.3\epsilon Cd}) \qquad (20)$$

where I_0 is the intensity of the incident light, Φ is the quantum yield of reaction, C is the concentration (of the charge-transfer complex), and d is the optical path length.[46] On the right side of eq 20, R_0 represents the rate when all the light is absorbed. Combining eq 2 with eq 20 leads to

$$-\ln\left(1 - \frac{R}{R_0}\right) = 2.3\epsilon K_{CT} d[R_4Sn][TCNE] \qquad (21)$$

Indeed, the rate of radical production R is linear with TCNE concentration and passes through the origin as shown in Figure 10. The magnitude of $K_{CT} = 1.1$ obtained from the slope and ϵ 77 M^{-1} cm^{-1} compares with the value of 0.65 in Table I obtained spectrophotometrically. The correspondence is surprisingly good if one considers the approximations and the differences in experimental conditions available for this comparison.[47]

Radicals produced during charge-transfer excitation must be intermediates in photoinsertion since the quantum yield of 0.2, measured as a lower limit for radical production in a frozen matrix at −175 °C, is still rather large and approaches the quantum yield of one, measured in solution for the photoinsertion process itself.[48] These observations are readily accounted for by the sequence of steps described in eq 15 and 16. Photoinsertion must then follow directly from the cage collapse of these fragments formed in eq 19, i.e.[49]

$$[R \cdot\ R_3Sn^+\ TCNE^- \cdot] \xrightarrow{\text{fast}} [R_3Sn\text{-}TCNE\text{-}R] \qquad (22)$$

The mechanism of photoinsertion is thus represented by the sequence of reactions given by eq 15, 16, 19, and 22.

3. Thermal Activation of Insertion. The observed second-order kinetics indicates that both alkylmetal and TCNE are present in the rate-limiting step for insertion. The importance of electron transfer in the transition state is reflected in the parallel relationship between the thermal rates of insertion (i.e., log k_T in eq 7) and the energetic of electron detachment measured independently by the ionization potentials (e.g., see Figure 13[50]).

The potential energy diagrams in Figure 11 illustrate how photoactivation via the charge-transfer transition $h\nu_{CT}$ is related to the thermal activation, designated as E_T. Indeed, among a limited series of methylethyllead compounds with similar steric properties, there is a reasonable linear relationship between $h\nu_{CT}$ and log k_T for photochemical and thermal insertion, respectively, as illustrated in Figure 12. A similar general trend in this correlation also pertains to the alkyltin analogues examined here. This correlation, coupled with the relationship observed between log k_T and the K_{CT}, leads us to the conclusion that electron transfer proceeds from the same charge-transfer complex

$$[R_4Sn\ TCNE] \xrightarrow{E_T} [R_4Sn^+ \cdot\ TCNE^- \cdot] \qquad (23)$$

which was proven to be directly involved in photochemical activation. The subsequent reactions leading to insertion are the same as the rapid dark reactions in eq 19 and 22 presented for the photoinduced insertion. Accordingly, thermal and photoactivation of insertion share common mechanistic pathways. Any difference may lie in the nature of the paramagnetic ion pair resulting from electron transfer within the charge-transfer complex as represented in eq 18 and 23.

4. Ion Pairs as Common Intermediates in Thermal and Photochemical Insertion. The Franck-Condon limitations placed on the photoinduced electron transfer in eq 18 restrict the intermolecular separation in the excited ion pair to that of the charge-transfer complex. In the thermal process, the same or a similar ion pair is also an intermediate derived by electron transfer in eq 23. Since these paramagnetic ion pairs are formed subsequent to the rate-determining step, their properties are best examined either by direct spectroscopic examination or by product selectivity.

Our attempts to observe the triplet ESR spectrum of the ion pair, produced either thermally or photochemically in solution or in a frozen matrix, were all consistently unsuccessful. The

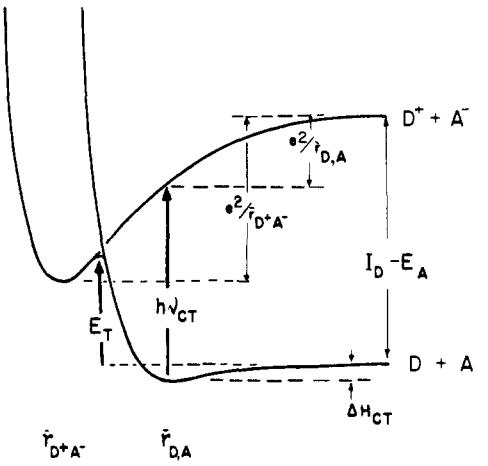

Figure 11. The relationship between thermal (E_T) and photochemical ($h\nu_{CT}$) activation of electron transfer proceeding from the charge-transfer complex.

negative results of the CIDNP studies also point out that the $R_4Sn^{+}\cdot$ moiety is very short lived.[51]

The direct comparison between the thermally and the photochemically induced formation of the ion pair, however, can be made by examining the selectivity in the fragmentation patterns of the alkyltin moiety prior to insertion. For example, the insertion into either the Me-Sn or the Et-Sn bond in the series of methylethyltin compounds is governed by the scission of the relevant bond in the paramagnetic alkyltin moiety represented as eq 24. The extent to which fragmentation of this

$$R_3\overset{+}{Sn}\begin{cases}Et \\ Me\end{cases}\begin{cases}\longrightarrow Et\cdot + MeSnR_2^{+} & (24a)\\ \longrightarrow Me\cdot + EtSnR_2^{+} & (24b)\end{cases}$$

cation radical proceeds from an excited state or from a geometrically distorted configuration or is influenced by $TCNE^{-}\cdot$, its counterion within the cage, would be reflected in changes in ethyl/methyl selectivity for insertion. The striking similarities of S(Et/Me) for both the thermal and photochemical processes strongly suggest that insertion proceeds from more or less the same paramagnetic ion pair.[52,53]

It is noteworthy that this selectivity is reasonably close to that (~9) observed in the unimolecular fragmentation of the molecule ion generated upon electron impact (EI) in the gas phase[32,33,54] (eq 25). The preferential scission of the Et-Sn

$$R_3Sn\begin{cases}Et \\ Me\end{cases}\xrightarrow[(EI)]{-\epsilon}\begin{cases}\longrightarrow Et\cdot + MeSnR_2^{+} & (25a)\\ \longrightarrow Me\cdot + EtSnR_2^{+} & (25b)\end{cases}$$

compared to the Me-Sn bond in the cation radical is in accord with their expected relative strengths evaluated from the mean bond energies for Et_4Sn and Me_4Sn of 46 and 56 kcal mol^{-1}, respectively.[55]

The observation of stable TCNE radicals in solution either as $TCNE^{-}\cdot$ or $R_3SnTCNE\cdot$ arises by a side reaction. Integration of the ESR signal indicates that these species generally constitute <0.1% of the reaction. However, measurement of the ESR line width dependence of TCNE radicals as a function of TCNE concentration indicates that they can undergo exchange at rates of 3×10^9 M^{-1} s^{-1},[27b,56] Similar exchanges lead to broadening of the NMR lines in the absence of an acetic acid quench. According to the scheme presented in eq 19 and 22, these radicals arise from partial diffusive separation from the cage, i.e.

$$[R\cdot\ R_3Sn^{+}\ TCNE^{-}\cdot] \xrightarrow{\text{diffuse}} R_3SnTCNE\cdot + R\cdot, \text{ etc.} \quad (26)$$

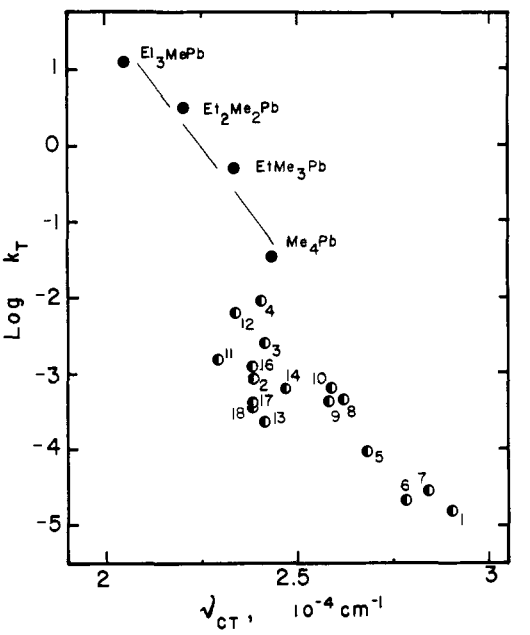

Figure 12. The correlation between the frequency of the charge-transfer band and the thermal rates of insertion of (●) methylethyllead and (◐) tetraalkyltin compounds (denoted by numbers in Table I).

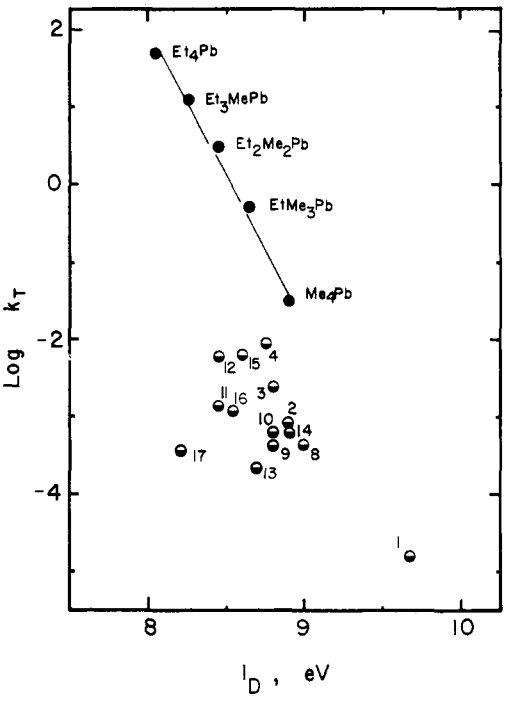

Figure 13. Steric effects in the correlation of the thermal rates of insertion and the ionization potentials of tetraalkyltin designated by numbers in Table I. Comparison with methylethyllead compounds.

Unfortunately, our attempts to observe CIDNP effects associated with such a competition have been unsuccessful as yet.

5. Steric Effects in Electron Transfer from Charge-Transfer Complexes. If the ion pairs described in the preceding section resulted from simple electron transfer between alkyltin and TCNE, it is expected that the rates (log k_T) would correlate linearly with the ionization potentials of the alkyltin compounds. Indeed, such a linear correlation can be observed in Figure 13 for the insertion reaction with a limited series of methylethyllead compounds with similar steric properties. If

the correlation is extended to the greater variety of alkyltin structures available in this study, it shows the same general trend, but with considerable scatter. However, a closer examination of the data reveals that deviations are systematic and most marked with sterically hindered compounds, decreasing roughly in the order t-Bu > i-Bu > i-Pr > Et ≫ Me. Tetraneopentyltin, the most sterically hindered compound, does not react at all.

The same general steric effects are shown in the correlation of log k_T with the charge-transfer frequency ν_{CT} in Figure 12, and lends further support to the charge-transfer complex as an intermediate in both thermal and photochemical insertions. The intermolecular distance between R_4Sn and TCNE in the transition state for electron transfer must be sufficiently small to allow for these variations. Indeed, a comparison with the inner-sphere pathway for electron transfer between the same alkyltin compounds and hexachloroiridate(IV) suggests that TCNE may have penetrated the coordination sphere of alkyltin sufficiently to cause significant distortion of the tetrahedral tin structure.[53]

Summary and Conclusion

The insertion reaction of alkylmetals and TCNE represents the first system in which the mechanism of thermal as well as photochemical activation can be separately and simultaneously examined in a charge-transfer process. The measurement of the formation constant K_{CT} and the extinction coefficient ϵ_{CT} of the charge-transfer complex allows steric effects to be evaluated quantitatively. Coupled with the identification of electron transfer for the charge-transfer complex as the activation step, a unified mechanism can be described for thermal and photochemical insertion in which all other intermediates are also shared in common. Thus, the same paramagnetic ion pair results from thermal and photochemical electron transfer, and it subsequently undergoes spontaneous scission to a caged radical pair observable by ESR only in a frozen matrix. Cage collapse of these fragments leads directly to insertion. Selectivity studies and steric effects provide important probes for the properties of the ion pair.

Experimental Section

Materials. The series of symmetrical tetraalkyltin compounds used in this study was prepared according to standard procedures.[57] A typical example follows. Stannic chloride (70 g, 0.27 mol) was added dropwise to 1.5 mol of EtMgBr in ether under a nitrogen atmosphere. The reaction mixture was refluxed for 4 h after the addition was completed and hydrolyzed with dilute (0.1 N) aqueous HCl. After repeated extractions with ether, the combined ethereal layer was finally washed with saturated $NaHCO_3$ and dried over $CaCl_2$. Distillation following the removal of solvent afforded Et_4Sn, bp 84 °C (11 mm).[57] Others follow: R_4Sn (bp) Me_4Sn (78 °C, 758 mm),[57] n-Pr_4Sn (79 °C, 2 mm),[57] i-Pr_4Sn (102 °C, 30 mm),[57] n-Bu_4Sn (92 °C, 1 mm),[57] i-Bu_4Sn (101 °C, 1.5 mm),[57] sec-Bu_4Sn (108 °C, 0.8 mm),[58] and neo-$Pent_4Sn$ (mp 124 °C after three recrystallizations from n-hexane).[59]

The unsymmetrical tetraalkyltin compounds, $RSnMe_3$ and R_2SnMe_2, were prepared by a similar procedure starting with Me_3SnCl and Me_2SnCl_2, respectively. Trimethyltin chloride was prepared either from Me_4Sn by HCl cleavage or by syn proportionation with a stoichiometric amount of $SnCl_4$. Dimethyltin dichloride was prepared from Me_4Sn and $SnCl_4$ at 130 °C for 4 h. Triethyltin chloride was prepared from Et_4Sn and acetyl chloride in the presence of aluminum chloride. $RSnMe_3$ (bp): $EtSnMe_3$ (105 °C, 760 mm),[57] n-$PrSnMe_3$ (131 °C, 760 mm),[60] i-$PrSnMe_3$ (123 °C, 120 mm),[61] n-$BuSnMe_3$ (150 °C, 750 mm),[57] t-$BuSnMe_3$ (56 °C, 36 mm).[62] R_2SnMe_2 (bp): Et_2SnMe_2 (65 °C, 50 mm),[60] n-Pr_2SnMe_2 (74 °C, 30 mm),[60] i-Pr_2SnMe_2 (66 °C, 30 mm),[57] n-Bu_2SnMe_2 (70 °C, 4 mm).[57] t-Bu_2SnMe_2 (75 °C, 30 mm).[57,63] i-Bu_2SnEt_2[57] was prepared from i-BuMgCl and Et_2SnCl_2 (from Et_4Sn and $SnCl_4$) (bp 124 °C, 13 mm).

Tetracyanoethylene from Du Pont was resublimed in vacuo before use. Acetonitrile (Mallinckrodt, analytical reagent) was stirred with calcium hydride overnight, filtered, and then distilled from P_2O_5 under a nitrogen atmosphere. Tetrahydrofuran was transferred in vacuo from a solution containing benzophenone ketyl. Chloroform and 1,2-dichloropropane were purified by successive washing with concentrated H_2SO_4, 5% $NaHCO_3$, and distilled water followed by drying over $CaCl_2$. They were then distilled from CaH_2 in a nitrogen atmosphere. Potassium ferrioxalate was synthesized by the literature procedure[64] and recrystalized from hot water three times.

Charge-Transfer Spectra of Alkyltin Compounds and TCNE. A solution of 0.01 M TCNE in chloroform or 1,2-dichloropropane contained in a 10-mm quartz cuvette was equilibrated in a thermostated compartment of a Cary 14 spectrophotometer. The alkyltin compound (5-400 μL) was added by means of a microsyringe and rapidly mixed. With most alkyltin, the absorption spectrum measurably decreased within a few minutes and necessitated rapid measurement of the spectrum. However, reproducibility to within 5% could be readily achieved.

To measure changes in TCNE concentration, the spectrum of a 5-11 × 10^{-4} M solution in 1,2-dichloropropane was first recorded. The alkyltin (7-50 μL) was then added to both the cuvette containing the sample as well as to the reference cell. The TCNE absorption decreased instantly upon the addition and in proportion to the amount of alkyltin added. Thereafter it remained constant for several minutes.

Kinetics of the Thermal Insertion Reaction. A 10-mm cuvette containing a solution of TCNE in acetonitrile was placed in a thermostated compartment of a Cary 14 spectrophotometer. The reaction was started by injecting 2-100 μL of tetraalkyltin by means of a microsyringe with shaking. The decrease in absorbance at 270.5 nm (ε 15 500) was followed. Tetraalkyltin used in this study does not absorb in this region.

Similar results could be obtained with the less reactive alkyltin compounds by observing the changes in the ^1H NMR spectra as described in more detail for the selectivity studies below.

Insertion Products of Tetraalkyltin and TCNE. The 1:1 insertion adducts of tetraalkyltin and TCNE are analogous to those found and characterized for the related tetraalkyllead compounds.[5] The relevant ^1H NMR data for Me_4Sn are δ 0.06 (s), and for the adduct $Me_3Sn(TCNE)Me$, Me-C, δ 2.08 (s, 1 H) and Me_3Sn, δ 0.70 (s, 3 H). For Et_4Sn, δ 0.97 (q, J = 7.5 Hz) and 1.35 (t, J = 7.5 Hz); for the adduct $Et_4Sn(TCNE)Et$, CH_3-C, δ 2.35 (q, 2 H, J = 7 Hz), CH_2, δ 1.43 (t, 3 H, J = 7 Hz), and Et_3Sn, δ 1.38 (s, 15 H).

Selectivity Studies in the Thermal Insertion Reactions with Methylethyltin Compounds. A sample of $EtMe_3Sn$ or Et_2Me_2Sn was added with the aid of a microsyringe to a CD_3CN solution (500 μL) of TCNE contained in an NMR tube, and immediately degassed by a freeze-pump-thaw cycle. The thermal reactions were carried out at 22 and 40 °C. The ^1H NMR data for the reactants and products are summarized. Et_2Me_2Sn: δ 0.10 (s, 3 H), 0.80 (q, 2 H, J = 8 Hz), 1.23 (t, 3 H, J = 8 Hz). Product mixture containing $Et(TCNE)SnEtMe_2$ and $Me(TCNE)SnMeEt_2$: δ 0.68 (s), 1.39 (s), 1.39 (t, J = 7 Hz), 2.20 (s), 2.43 (q, J = 7 Hz). $EtMe_3Sn$: δ 0.10 (s, 9 H), 0.80 (q, 2 H, J = 8 Hz), 1.23 (t, 3 H, J = 8 Hz). Product mixture of $Et(TCNE)SnMe_3$ and $Me(TCNE)SnEtMe_2$: δ 0.70 (s), 1.39 (s), 1.39 (t, J = 7 Hz), 2.18 (s), 2.42 (q, J = 7 Hz).

The selectivities were determined from the ratio of intensities of the trialkyltin fragments in the adducts in the following manner. For Me_3EtSn, the selectivity was obtained from the ratio of the intensity of the resonance due to the Me group in 1,1,2,2-tetracyanobutanide (i.e., the lowest field peak of the triplet at δ 1.39) to the resonance at δ 1.39 comprising the central peak of the triplet (δ 1.39) for the Me group in 1,1,2,2-tetracyanobutanide and the resonance due to the ethyl group in the $EtSnR_2$ moiety. The selectivity $S(Et/Me) = 20c/(1 - 2c)$, where c = (lowest magnetic field triplet at δ 1.39)/(central resonance at δ 1.39 comprised of the central peak plus the Et contribution). For Et_2Me_2Sn, the ratio of the resonance at δ 1.39 (s and t) to that at δ 2.43 (q) was used. Four ratios were considered: let a = [MeR_2Sn (δ 0.70)]/[EtR_2Sn (δ 1.39)], then $(5a - 6)/(3 - a)$ = $S(Et/Me)$ for Me_3SnE and $(10a - 3)/(6 - 8a)$ = $S(Et/Me)$ for Me_2SnEt_2. Similarly, let b = [EtR_2Sn (δ 1.39)]/[CH_2 in adduct (δ 2.42)]; then $15/(2b - 3)$ = $S(Et/Me)$ for $EtMe_3Sn$ and $5/(b - 4)$ = $S(Et/Me)$ for Me_2SnEt_2. Also, let c = (lowest magnetic field peak at δ 1.39)/(center resonance at δ 1.39); then $20c/(1 - 2c)$ = $S(Et/Me)$ for $EtMe_3Sn$ and $40c/(3 - 26c)$ = $S(Et/Me)$ for Et_2Me_2Sn. Table II shows the consistency of the results. It should be emphasized,

however, that S(Et/Me) measured in this difficult manner is reliable to only one significant figure (±10%).

Chemically Induced Dynamic Nuclear Polarization Studies. A sample of alkyltin was added with the aid of a microsyringe to an NMR tube containing 0.16 M TCNE in CD_3CN under argon. The reaction was sufficiently slow with Et_4Sn to observe the changes in the NMR spectrum at 35 °C. Since the insertion reaction with Et_4Pb occurs on mixing, the components were mixed at −30 °C and then transferred to the spectrometer. As the temperature of the probe was raised gradually, the spectral changes could be followed. The effect of the magnetic field was also examined by mixing at various distances from the NMR probe or within a permanent magnet (300 G) and by varying the distance from 5 to 10 cm. Upon mixing, the tubes were immediately transferred to the NMR probe and scanned at 10-s intervals. Although a strong emission could be observed for the reaction of isopropyl iodide and sodium naphthalene in dimethoxyethane as reported by Garst and co-workers,[28] no CIDNP was observed between TCNE and tetraethyltin or lead.

Electron Spin Resonance Measurements. The alkyltin compound was added to a TCNE solution prepared from either 1,2-dichloropropane or acetonitrile and thoroughly degassed in vacuo. The ESR spectrum taken on a Varian E-112 X-band spectrometer was calibrated with a ^1H NMR field marker. The radical concentration was determined by double integration using DPPH as a calibrant (±15%). The relative concentrations were readily measured to within 5%.

The photochemical experiments were carried out in a mixed solvent consisting of 1:1 v/v acetonitrile and 1,2-dichloropropane to increase solubility. The alkyltin compound was added to a precooled, degassed solution of TCNE. The solution was then subjected to three freeze-pump-thaw cycles before sealing. The quartz tube was then placed in the ESR cavity at −175 °C and irradiated with light from a 1-kW high-pressure mercury lamp using either of the three filters described in Figure 6.

Photochemically Induced Insertion Reaction. A thoroughly degassed and evacuated solution of alkyltin and TCNE in acetonitrile prepared as described above was transferred to a transparent Dewar maintained at −35 °C with a stream of cooled nitrogen. Irradiation was carried out with filtered light from a 1-kW high-pressure mercury lamp transmitting at 436 nm, typically for 5–10 h. After reaction, the tube was cooled to −135 °C and the yield of TCNE radicals determined by ESR. The yield of insertion product was measured by integrating its ^1H NMR spectrum: e.g., the NMR spectrum of the Me_4Sn adduct consisted of δ 0.69 (s, 3 H) and 2.16 (s, 1 H). However, the thermal reaction of Et_4Sn was too fast to monitor in this manner, and the progress of reaction was followed by the disappearance of TCNE.

The light intensities for all the photochemical experiments were measured with ferrioxalate as an actinometer.[64] The intensities, accurate to ±10%, were repeatedly calibrated for the experimental setup employed, before and after reaction.

Acknowledgment. We wish to thank Professor M. Tamres for helpful discussions on the determination of the formation constants for weak complexes and for a preprint of his review, M & T Chemical Co. for a generous gift of stannic chloride, Professor M. Weiner for the measurement of some of the ionization potentials of tetraalkyltin, and the National Science Foundation for financial assistance.

References and Notes

(1) M. H. Abraham in "Comprehensive Chemical Kinetics", Vol. 12, C. H. Bamford and C. F. H. Tipper, Eds., Elsevier, Amsterdam, 1972.
(2) (a) R. Foster, "Organic Charge Transfer Complexes", Academic Press, New York, 1969; (b) R. Foster, Ed., "Molecular Complexes", Vol. 2, Crane Russak and Co., New York, 1974, p 108.
(3) V. F. Traven and R. West, *J. Am. Chem. Soc.*, **95**, 6824 (1973).
(4) H. Sakurai, M. Kira, and T. Uchida, *J. Am. Chem. Soc.*, **95**, 6826 (1973).
(5) H. C. Gardner and J. K. Kochi, *J. Am. Chem. Soc.*, **98**, 2460 (1976).
(6) J. Y. Chen, H. C. Gardner, and J. K. Kochi, *J. Am. Chem. Soc.*, **98**, 6150 (1976).
(7) M. F. Lappert and B. Prokai, *Adv. Organomet. Chem.*, **5**, 225 (1967).
(8) Cf. also S. D. Ittel and J. A. Ibers, *Adv. Organomet. Chem.*, **14**, 33 (1976).
(9) K. Mochida, J. K. Kochi, K. S. Chen, and J. K. S. Wan, *J. Am. Chem. Soc.*, **100**, 2927 (1978), is a preliminary report of this study.
(10) A. K. Colter and M. R. J. Dack in "Molecular Complexes", Vol. 1, R. Foster, Ed., Crane Russak and Co., New York, 1973, p 363 ff.
(11) M. Tamres and R. L. Strong in "Molecular Association", Vol. 2, R. Foster, Ed., Academic Press, New York, 1979.
(12) N. Mataga and T. Kubota, "Molecular Interactions and Electronic Spectra", Marcel Dekker, New York, 1970.
(13) R. S. Mulliken and W. B. Person, "Molecular Complexes, a Lecture and Reprint Volume", Wiley-Interscience, New York, 1969.
(14) (a) H. A. Benesi and J. H. Hildebrand, *J. Am. Chem. Soc.*, **71**, 2703 (1949); (b) R. M. Keefer and L. J. Andrews, *ibid.*, **77**, 2164 (1955).
(15) L. E. Orgel and R. S. Mulliken, *J. Am. Chem. Soc.*, **79**, 4839 (1957).
(16) Cf. also P. R. Hammond, *J. Chem. Soc. A*, 3025 (1971); P. R. Hammond and L. A. Burkardt, *J. Phys. Chem.*, **74**, 639 (1970).
(17) For a summary of weak 1:1 complexes and 1:1 contacts, see the excellent recent review in ref 11.
(18) E. Ciganek, W. J. Linn, and O. W. Webster in "The Chemistry of the Cyano Group", Z. Rappoport, Ed., Interscience, New York, 1970, Chapter 9.
(19) It should be noted that, if adventitious impurities in R_4Sn reacted with TCNE, the decrease in absorbance would depend only on the alkyltin concentration, and the value of $(A'_0/(A'_0 - A'))$ should be proportional to the TCNE concentration.
(20) As the absorption due to TCNE disappeared, no new peak was observed above 230 nm. We conclude that it was shifted to lower wavelengths. Similar blue shifts accompanying the formation of CT complexes have been noted.[21]
(21) (a) T. Kubota, *J. Am. Chem. Soc.*, **87**, 458 (1965); (b) S. Iwata, J. Tanaka, and S. Nagakura, *ibid.*, **88**, 894 (1966); (c) W. M. Moreau and K. Weiss, *ibid.*, **88**, 204 (1966); (d) M. Tamres and S. N. Bhat, *ibid.*, **95**, 2516 (1973), and related papers.
(22) W. B. Person, *J. Am. Chem. Soc.*, **87**, 167 (1965).
(23) P. J. Krusic, H. Stoklosa, L. E. Manzer, and P. Meakin, *J. Am. Chem. Soc.*, **97**, 667 (1975).
(24) (a) E. Samuel, D. Vivien, and J. Livage, *Inorg. Chim. Acta*, **21**, 179 (1977); (b) M. P. Eastman, D. A. Ramirez, C. D. Jaeger, and M. T. Watts, *J. Phys. Chem.*, **80**, 182 (1976).
(25) A. B. Cornwell, P. G. Harrison, and J. A. Richards, *J. Organomet. Chem.*, **140**, 273 (1977).
(26) It should be noted that the coupling constant obtained by averaging the three nitrogen splittings (i.e., $\bar{a}_{N_{1,2,3}} = 1.69$ G) is identical with that obtained from a sharp, well-resolved spectrum of $TCNE^{-\cdot}$ in solution.
(27) P. H. Kasai, *Acc. Chem. Res.*, **4**, 329 (1971); (b) M. T. Watts, M. L. Lu, R. C. Chen, and M. P. Eastman, *J. Phys. Chem.*, **77**, 2959 (1973).
(28) J. F. Garst, R. H. Cox, J. T. Barbas, R. D. Roberts, J. I. Morris, and R. C. Morrison, *J. Am. Chem. Soc.*, **92**, 5761 (1970).
(29) (a) R. W. Fessenden and R. H. Schuler, *J. Chem. Phys.*, **39**, 2147 (1963); (b) P. B. Ayscough and C. Thomson, *Trans. Faraday Soc.*, **58**, 1477 (1962).
(30) C. L. Wong, K. Mochida, J. K. Kochi, and M. Weiner, *J. Org. Chem.*, in press.
(31) (a) J. H. D. Eland, *Int. J. Mass Spectrom. Ion Phys.*, **4**, 37 (1970); B. G. Cocksey, J. H. D. Eland, and C. J. Danby, *J. Chem. Soc., Faraday Trans. 2*, **69**, 1558 (1973); (b) T. P. Fehlner, J. Ulman, W. A. Nugent, and J. K. Kochi, *Inorg. Chem.*, **15**, 2544 (1976).
(32) (a) S. Boué, M. Gielen, and J. Nasielski, *Bull. Soc. Chim. Belg.*, **77**, 43 (1968). (b) Cf. also B. G. Hobrock and R. W. Kiser, *J. Phys. Chem.*, **66**, 155 (1962); V. H. Dibeler, *J. Res. Natl. Bur. Stand.*, **49**, 235 (1952).
(33) C. L. Wong and J. K. Kochi, *J. Am. Chem. Soc.*, **101**, 5593 (1979).
(34) (a) R. S. Mulliken, *J. Am. Chem. Soc.*, **74**, 811 (1952); (b) M. Tamres and J. Grundnes, *ibid.*, **93**, 801 (1971). (c) Insofar as it is applicable to weak complexes as well as contacts.
(35) Strictly speaking, the linear correlation does not require the electrostatic term to be constant. It may be proportional to I_D.
(36) Quantification of the effect would require a knowledge of the structures of these 1:1 complexes. However, we are tempted in suggesting that the principal twofold axes of TCNE and R_2Hg are mutually perpendicular, but offset to allow maximum overlap of the p and π^* orbitals.
(37) For a quantitative measure of steric effects for alkyl groups, see J. A. MacPhee, A. Panaye, and J.-E. Dubois, *Tetrahedron Lett.*, 3293 (1978).
(38) (a) The same applies if other slopes are considered, provided there is no (unreasonable) change in sign. (b) The various alkyl substitution patterns on the tin center do not allow a more extensive discussion of the steric effects at this juncture.
(39) The curves are drawn according to Kosower[40] so that the mean intermolecular distance in the ion pair is less than that in the weak, uncharged complex.
(40) E. M. Kosower, *Prog. Phys. Org. Chem.*, **3**, 81 (1965).
(41) In the usual treatment,[42] the vibrational transition probability is allowed and taken as unity. However, it is more forbidden in σ–π complexes of the type examined here owing to poor orbital overlap.
(42) Cf. M. W. Hanna and J. L. Lippert, *Mol. Complexes*, **1**, 1 (1973).
(43) A. K. Colter and M. R. J. Dack, *Mol. Complexes*, **2**, 1 (1974).
(44) Although very likely, it does not *prove* it since K_{CT} is of limited magnitude.
(45) Cf. D. O. Cowan and R. L. Drisko, "Elements of Organic Photochemistry", Plenum Press, New York, 1976.
(46) The exponential term in eq 20 is estimated to be 0.011 ($\ll 1$) from the data in Table I.
(47) For example, the K_{CT} in eq 21 is obtained at −175 °C in a frozen matrix, whereas the value in Table I is determined at 30 °C in solution. For these complexes, ΔH_{CT} is small, having a measured value of 0.9 ± 0.3 kcal mol^{-1} for Et_4Sn between 0 and 34 °C.
(48) The quantum yield for radical production does not include those radicals lost by very rapid cage combinations as well as light loss due to reflection from the frozen matrix.
(49) It may proceed either by initial radical combination followed by ion pair collapse such as $[R\cdot\ R_3Sn^+\ TCNE^{-\cdot}] \rightarrow [R_3Sn^+\ TCNE(R)^-] \rightarrow R_3Sn$–TCNE(R), or via the reverse sequence of steps involving ion pairing followed by radical combination.
(50) The plot is linear for a series of alkyllead compounds with similar steric properties,[5] but shows systematic deviations in those alkyltin analogues with increased steric hindrance.
(51) (a) Furthermore, the large spin–orbit interactions for organotin compounds leading to short spin–spin relaxation times may also discourage polarization

of the nuclear spins. Alternatively, the efficiency of cage combination may be too high to allow sufficient S–T mixing to observe CIDNP. (b) The negative CIDNP results in various magnetic fields indicate that no $S-T_{-1}$ or $S-T_0$ mixing could be detected. (c) The fast electron transfer between $TCNE^{-}\cdot$ and TCNE in the order of $3 \times 10^9\ M^{-1}\ s^{-1}$ will also destroy spin correlation [cf. R. Kaptein, *Adv. Free-Radical Chem.*, **5**, 319 (1975)]. (d) Photo-CIDNP studies at low temperatures are in progress.
(52) Selectivities have been also measured for the same alkyltin compounds in electron transfer with iron(III) and iridate(IV)[30] and are diagnostic of the properties of the ion pair.[53]
(53) C. L. Wong, S. Fukuzumi, and J. K. Kochi, to be published.
(54) Cf. also (a) S. Boué, M. Gielen, J. Nasielski, J.-P. Lieutenant, and R. Spielmann, *Bull. Soc. Chim. Belg.*, **78**, 135 (1969); (b) for EI of related Me_2Hg see C. S. T. Cant, C. J. Danby, and J. H. D. Eland, *J. Chem. Soc., Faraday Trans. 2*, **71**, 1015 (1975).
(55) W. V. Steele, *Annu. Rep. Prog. Chem., Sect. A*, **71**, 103 (1974).
(56) Estimated in the fast exchange limit [cf. R. Chang and C. S. Johnson, Jr., *J. Chem. Phys.*, **46**, 2314 (1967)].
(57) R. K. Ingham, S. D. Rosenberg, and H. Gilman, *Chem. Rev.*, **60**, 459 (1960), and references cited therein.
(58) W. P. Neumann, B. Schneider, and R. Sommer, *Justus Liebigs Ann. Chem.*, **692**, 1 (1966).
(59) H. Zimmer, I. Hechenbleikner, O. A. Homberg, and M. Danzik, *J. Org. Chem.*, **29**, 2632 (1964).
(60) F. H. Pollard, G. Nickless, and D. N. Dolan, *Chem. Ind. (London)* 1027 (1965).
(61) S. Boué, M. Gielen, and J. Nasielski, *J. Organomet. Chem.*, **9**, 443 (1967).
(62) R. C. Putnam and H. Pu, *J. Gas Chromatogr.*, **3**, 160 (1965).
(63) S. A. Kandil and A. L. Allred, *J. Chem. Soc. A*, 2987 (1970).
(64) C. G. Hatchard and C. A. Parker, *Proc. R. Soc. London, Ser. A*, **235**, 58 (1956).

Control of Regioselectivity in the Di-π-methane Rearrangement. Triplet-Sensitized Photoisomerization of Benzonorbornadienes Carrying Cyano Substituents in the Aryl and Vinyl Segments

Leo A. Paquette,* Audrey Yeh Ku, Cielo Santiago, Melvin D. Rozeboom, and K. N. Houk*

Contribution from the Evans Chemical Laboratories, The Ohio State University, Columbus, Ohio 43210, and the Department of Chemistry, Louisiana State University, Baton Rouge, Louisiana 70803. *Received April 4, 1979*

Abstract: Triplet-sensitized irradiation of 2-cyanobenzonorbornadiene (**10**) gives rise exclusively to 3-cyanotetracyclo[5.4.0.0^{2,4}.0^{3,6}]undeca-1(7),8,10-triene (**30**). This strong preference for benzo-vinyl bridging to C_3 has also been observed in the case of the four possible aryl-substituted dicyano derivatives. In all of these examples, striking regiospecificity is exhibited, despite untoward aryl polar effects in two examples. This bonding preference is shown to conform to the vacant orbital energies and shapes present in the starting benzonorbornadienes as calculated by STO-3G procedures and supported by photoelectron spectroscopy. The synthetic approaches to the polar substituted benzonorbornadienes are also detailed.

The high propensity of benzo-fused bicyclic dienes for triplet-sensitized di-π-methane rearrangement has been well established during the last decade.[1] With benzonorbornadiene (**1**) as the illustrative example, light-induced isomerization can

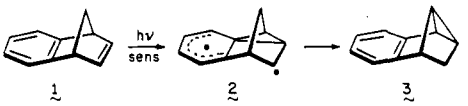

1 **2** **3**

be seen to involve initial intramolecular aryl-vinyl bridging and subsequent σ bond cleavage. Attachment of a substituent to the aromatic ring necessitates added consideration of regioselectivity. This is because **1** is a "doubly connected"[2] di-π-methane system, such that two regiochemically distinct bonding schemes are possible. Since conversion of biradical intermediates of type **2** to products has, in the many reported instances, been dominated completely by the exothermicity of rearomatization,[1] the observed product distribution is directly relatable to substituent control in the bridging step.

Previously, we reported on the striking control of bonding options observed during the photorearrangement of benzonorbornadienes substituted by electron donor and acceptor groups in the meta[3] and ortho positions.[4] In the case of meta acceptors, completely regiospecific para bridging was noted with ultimate formation of **4**. In contrast, meta donors directed matters predominantly through the alternate meta bridging channel to **5**. Interestingly, either type of ortho substituent

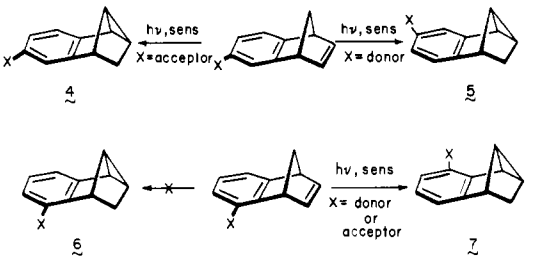

4 **5**

6 **7**

promoted benzo-vinyl bridging preferentially to the adjacent (ortho) aryl carbon to deliver chiefly **7**. These results have been concisely accounted for in terms of an MO model which attributes considerable importance to benzene HOMO and LUMO polarization.[4a,5]

The present research developed as a consequence of interest in the situation where two cyano substituents, one on the aryl ring and one on the vinyl moiety, would be allowed to vie for control of the bridging step. Hitherto, such competitive experiments had not been investigated.[6] The selection of cyano functionality for our initial studies was motivated by: (a) the unusually high regiocontrol noted earlier in the production of **4**-CN and **7**-CN, and (b) an earlier theoretical prediction that unsymmetrical substitution of the olefinic bond by an electron-withdrawing substituent should direct bridging away from the acceptor group because of the larger coefficient at the unsubstituted olefinic carbon in the LUMO.[5]

Results

Synthesis of the Dicyanobenzonorbornadienes. Access to the

*L. A. Paquette, The Ohio State University; K. N. Houk, Louisiana State University.

0002-7863/79/1501-5972$01.00/0